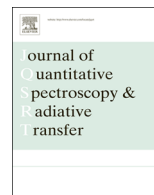




Contents lists available at ScienceDirect

# Journal of Quantitative Spectroscopy & Radiative Transfer

journal homepage: [www.elsevier.com/locate/jqsrt](http://www.elsevier.com/locate/jqsrt)

## Temperature dependences for N<sub>2</sub>- and air-broadened Lorentz half-width coefficients of methane transitions around 3.38 μm



Hongliang Ma<sup>a,d</sup>, Qiang Liu<sup>a</sup>, Zhensong Cao<sup>a,\*</sup>, Weidong Chen<sup>b</sup>, Aurore Vicet<sup>c</sup>, Yinbo Huang<sup>a</sup>, Wenyue Zhu<sup>a</sup>, Xiaoming Gao<sup>a</sup>, Ruizhong Rao<sup>a</sup>

<sup>a</sup> Key Laboratory of Atmospheric Composition and Optical Radiation, Chinese Academy Sciences, Hefei 230031, China

<sup>b</sup> Laboratoire de Physicochimie de l'Atmosphère, Université du Littoral Côte d'Opale, 189A, Av. Maurice Schumann, 59140 Dunkerque, France

<sup>c</sup> Université Montpellier 2, Campus St Priest, IES Institut d'Electronique et des Systèmes, 860 rue de St Priest, 34095 Montpellier Cedex 5, France

<sup>d</sup> University of Chinese Academy of Sciences, Beijing 100039, China

### ARTICLE INFO

#### Article history:

Received 31 August 2015

Received in revised form

2 December 2015

Accepted 4 December 2015

Available online 12 December 2015

#### Keywords:

Methane

IR laser

Mid-infrared absorption spectroscopy

Temperature dependence exponent

Pressure-broadened half-width coefficient

### ABSTRACT

We have measured high-resolution absorption spectra of methane broadened by N<sub>2</sub> and air at sample temperatures between 173.0 K and room temperature. The measurements were performed based on direct laser absorption spectroscopy using a tunable diode laser combined with a temperature controlled cryogenically cooled absorption cell. These spectra have been analyzed to determine the pressure-broadened half-width coefficients as well as their temperature dependences for six singlet lines belonging to the ν<sub>3</sub> band of methane near 3.38 μm. To our knowledge, the temperature dependence exponents for the pressure-broadened half-width coefficients are reported experimentally for the first time for six transitions of <sup>12</sup>CH<sub>4</sub> with intensities stronger than 4 × 10<sup>-20</sup> cm<sup>-1</sup>/(molecule cm<sup>-2</sup>). The measured half-width coefficients and the temperature dependence exponents of these transitions are compared with the available values reported in the literature and the HITRAN2012 database. Agreements and discrepancies are discussed.

© 2015 Elsevier Ltd. All rights reserved.

## 1. Introduction

Methane is an important trace constituent and a greenhouse gas of the Earth's atmosphere, and also present in the outer planets and Titan's atmosphere [1]. Its concentration has significantly increased due to human activities on the Earth's environment since the last century. Precise knowledge of the spectroscopic line parameters are key to infrared remote sensing of CH<sub>4</sub> of the atmospheres for the earth and the outer planets [2,3] which will help scientists understand its atmospheric evolution, and accurate interpretation of

infrared observations of terrestrial and extraterrestrial atmospheres [4].

In the near infrared region, CH<sub>4</sub> spectrum at room temperature and low temperature are extensively studied by many groups [5–10]. In the mid-infrared region, for instance, CH<sub>4</sub> spectra in the ν<sub>3</sub> band contains many strong absorption lines which are very important for trace gas detection [11] and the Earth's radiation balance [12]. In order to fulfill the requirement of these important applications, precise line parameters (i.e. positions, intensities, broadening coefficients and temperature dependence exponents) of the spectral lines are required, especially the temperature dependence exponents because of the wide temperature range in the earth and other planetary atmospheres. Previously, the line parameters of CH<sub>4</sub> in this band have been studied by Benner et al. [13], Pine [14] and

\* Corresponding author.

E-mail address: [zscao@aiofm.ac.cn](mailto:zscao@aiofm.ac.cn) (Z. Cao).

Pine and Gabard [15] but all studies were performed at room temperature. To the best of our knowledge, three papers reported high resolution work on the  $\nu_3$  band of  $\text{CH}_4$  at low temperature [16–18]. In 1979, the air temperature dependence exponents of three lines ( $R(0)$ ,  $R(1)$  and  $R(2)$ ) have been reported by Varanasi [16]. Later, in 1983, Devi et al. [17] have published the temperature dependence of nitrogen-broadened half-widths of  $^{12}\text{CH}_4$  in the  $\nu_3$  band from 2870 to 2883  $\text{cm}^{-1}$  with a tunable diode laser spectrometer. In 2007, the temperature dependence of the nitrogen broadening coefficients of four lines of the P9 manifold in the  $\nu_3$  band have been published by Mondelain et al. [18] for atmospheric purposes. In the 2726–3200  $\text{cm}^{-1}$  interval, the HITRAN2012 database (hereafter, shortened to "HITRAN") [19] has assumed the air-broadened temperature dependence exponents from Ref. [20], which calculated the pressure-broadened half-width and the pressure-induced line shift for roughly 4000 transitions with  $\text{N}_2$ ,  $\text{O}_2$  and air as the perturbing gases. The calculations were made at 225.0 and 296.0 K in order to determine the temperature dependence of the half-width. Besides these results, no further low temperature experimental information has been obtained for these lines, and hence the present measurements are important.

In the present study, a temperature controlled cryogenically cooled absorption cell combined with a narrow linewidth tunable diode laser were used to study six strong lines in the  $\nu_3$  band of methane near 3.38  $\mu\text{m}$  broadened by air and nitrogen at low temperature as well as room temperature. The temperature dependence exponent  $n$  and the pressure-broadened half-width coefficients for six transitions of  $^{12}\text{CH}_4$  with intensities stronger than  $4 \times 10^{-20} \text{ cm}^{-1}/(\text{molecule cm}^{-2})$  have been determined and compared with the available values reported in the literature and the HITRAN2012 database. Since the present study was focused on halfwidth coefficients and their temperature dependence exponents, other parameters are not provided in our final results.

## 2. Experiment details

The experimental setup is schematically shown in Fig. 1. The light source used was a continuous wave distributed feedback diode laser emitting radiation near 3.38  $\mu\text{m}$  with a relatively narrow linewidth of about 3 MHz, which can be neglected comparing to Doppler limited molecular absorption linewidth (for a  $\text{CH}_4$  line near 3.38  $\mu\text{m}$  at 296 K, the typical Doppler half-width at half-maximum is about 137 MHz). The typical power of the laser was about 1.1 mW; its temperature and current were driven by a low noise controller (ILX Lightwave LDC-3724C). The controller was linked to a computer via a GPIB interface. During the experiment, the laser temperature was fixed while its current was scanned in a step by step mode with typical step size of 0.1 mA in order to sweep the molecular transitions. The beam was split into three parts by a wedged  $\text{CaF}_2$  beam-splitter. The first part (about 90%) was introduced into a wavemeter (Bristol-621A IR) to record the frequency of the absorption lines with the repeatability of  $0.00018 \text{ cm}^{-1}$  and the uncertainty of  $0.0015 \text{ cm}^{-1}$  at 3.38  $\mu\text{m}$ . The second part (about 5%) passed through a room-temperature reference cell (30.7 cm) filled with pure  $\text{CH}_4$  at low pressure ( $< 0.5$  Torr) providing the reference signal. The third part (about 5%) propagated through the sample cell for the absorption signal. Two photodetectors (Vigo, PVI-4TE-4) were used to record the sample and the low-pressure reference spectra. Since the wavemeter needs adequate power for the wavelength readings and the detectors are very sensitive, therefore we arranged the 3 parts as mentioned above. The signals from the photodetectors were acquired via a DAQ card (NI, USB6356) by a computer using Labview software and then stored for post-processing analysis.

The temperature controlled low temperature absorption cell was previously described in Ref. [21]. Briefly, the optical path length of the sample cell is 17.4 cm. In order to get proper thermal uniformity, the cell body was made of

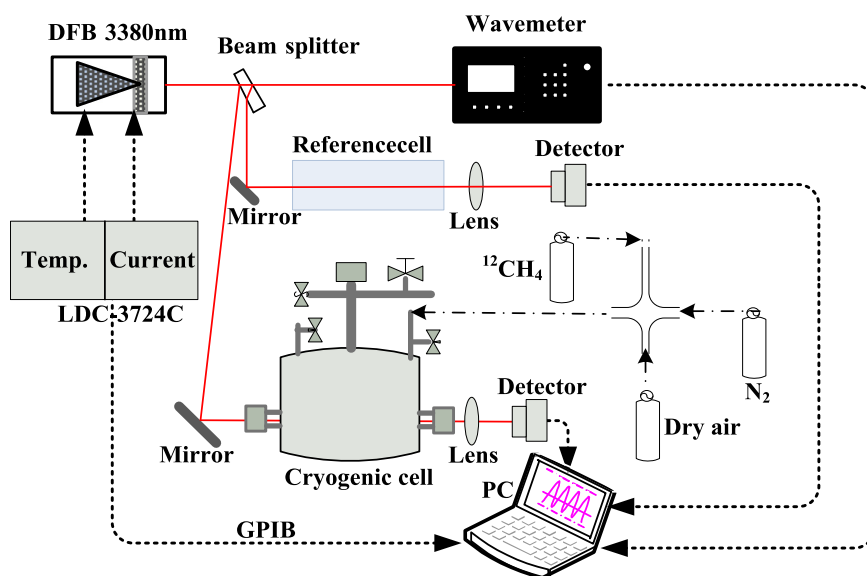


Fig. 1. Schematic of the experimental setup for the  $\text{CH}_4$  spectra measurement.

copper because of its high thermal conductivity. The entire sample cell and a two-liter liquid nitrogen storage dewar were enclosed in a external stainless steel cylinder with two CaF<sub>2</sub> windows (1 cm in diameter). An external vacuum chamber provides high vacuum integrity to isolate thermal conductivity. The temperature in the cell is monitored using two PT100 sensors mounted at different locations on the wall of the sample cell, while the sample cell can be controlled well from 150 K to room temperature with a stability of better than 0.3 K. The gas samples (methane, air, nitrogen) with a purity of 99.99% were used. The pressures of the gas mixtures were measured with a capacitance gauge (MKS 626C) with an accuracy of 0.25%.

### 3. Data processing

For a monochromatic laser beam, the transmission of light radiation  $T_\nu$  at a frequency  $\nu$  through a uniform gas can be given by the Lambert–Beer law

$$T_\nu = \frac{I_\nu(\nu)}{I_0} = e^{-\kappa(\nu)L} \quad (1)$$

where  $I_0$  and  $I_\nu(\nu)$  are referred to the incident and transmitted power, respectively,  $\kappa(\nu)$  (in [cm<sup>-1</sup>]) is the spectral absorption coefficient;  $L$  (in [cm]) is the optical path length within the cell.

To retrieve the Lorentz half-width coefficients of methane transitions, a nonlinear least-squares fitting (NLSF) method was used to determine the parameters by fitting the spectra to the Voigt profile, where the Doppler half-width  $\Delta\nu_D$  was fixed and the other parameters were adjusted by the computer, including line position, integrated area, line width, and the parameters for the base-line which was modeled by a third order polynomial.

For a given perturber, the collision half-width can be defined by:

$$\Delta\nu_L = P_{self} \cdot \gamma_{self} + P_{out} \cdot \gamma_{out} \quad (2)$$

where  $P_{self}$  is the partial pressure of methane,  $\gamma_{self}$  is the coefficient for self-broadening,  $P_{out}$  is the perturber (air or nitrogen) pressure,  $\gamma_{out}$  is the coefficient for collisional broadened by air and nitrogen.

The temperature dependence exponent of the measured half-width coefficients follows the relation

$$\gamma(T, P) = P\gamma(T_0, P_0) \left[ \frac{T_0}{T} \right]^n \quad (3)$$

where the reference pressure and temperature are  $P_0=1$  atm and  $T_0=296$  K, respectively. Here  $\gamma(T, P)$  is the measured half-width at pressure  $P$  and temperature  $T$ , and  $\gamma(T_0, P_0)$  is the half-width of the line at 1 atm pressure and reference temperature  $T_0=296$  K.

Fig. 2 presents an example of an absorption spectrum and the corresponding base line given by the fit. To fit the observed spectra for these transitions, a multi-peak fitting program was used, the spectrum parameters, including the line positions, the pressure-broadened width and the absorption coefficient, were obtained by using the multi-peak fitting program with the Voigt spectral profile. Note that the Doppler width was fixed at the calculated value

during the fitting. Fig. 3 shows an example of the absorption spectrum at 223.0 K which was broadened by air. As it is shown in Fig. 3, the multi-peak fitting program was well suited for the fitting, and the same procedure was also used for the following data processing.

## 4. Results and discussion

### 4.1. Air- and N<sub>2</sub>-broadening coefficients

During the measurements, the sample cell was first evacuated to the order of 10<sup>-4</sup> Torr using a mechanical together with a molecular pump (Leybold, TW300), then filled with the natural abundance CH<sub>4</sub> gas of 99.99% purity and air or N<sub>2</sub>. In order to mix the gases fully, signals were always recorded after at least 3 h of preparing the gas mixtures. Table 1 summarizes the experimental conditions for the entire set of spectra used in this work.

To obtain pressure-broadened half-width coefficients, we have recorded 3 or 4 spectra for each experimental condition. Using the NLSF fit of the spectral profile, the Lorentz half-width, can be derived from each spectrum. Because the fraction of CH<sub>4</sub> in the mixture gases was always less than 0.5 Torr, the Eq. (2) can be simply described by:

$$\Delta\nu_L = P_{out} \cdot \gamma_{out} \quad (4)$$

Using Eq. (4), the pressure-broadened half-width coefficients  $\gamma_0^{N_2}$  and  $\gamma_0^{air}$  were determined by plotting the Lorentz widths versus gas pressure and then fitting them by straight lines. The slopes of these lines give directly the broadening parameters for each spectral transition. Fig. 4 illustrates the individual air-broadening coefficient obtained for the transition at 2958.017263 cm<sup>-1</sup>, with different symbols indicating measurements at different temperatures. The temperature and pressure were varied between 173.0 and 296.0 K and from 50 to 350 Torr, respectively. The pressure-broadened half-width coefficients at various temperatures achieved in the present work are plotted against wavenumber values for 6 transitions are shown in Fig. 5. The error bars correspond to one standard deviation given by the linear regression of the present work. These errors represent only the uncertainties as obtained from the nonlinear least-squares fits and do not reflect the actual uncertainties. At the mean time, the systematic errors of the air- and N<sub>2</sub>-broadening coefficients arising from the choice of line profile model, frequency, pressure and temperature were also estimated according to Ref. [22], these systematic errors are difficult to assess, but are less than 5%, as stated from our experience. Accounting for the various errors, the maximum absolute errors in our measured parameters are estimated to be better than 8% for the N<sub>2</sub>- and air-broadening coefficients. Fig. 5 also shows that, the air-broadening coefficients (upper panel) are slightly smaller than N<sub>2</sub>-broadening coefficients (Lower panel), and the broadening coefficients at each temperature have the similar tendency.

Starting two decades ago, the air-, N<sub>2</sub>- and O<sub>2</sub>-broadening coefficients have been measured by Benner et al. [13] for more than 450 transitions in the  $\nu_3$  region of <sup>12</sup>CH<sub>4</sub>, between 2650 and 3200 cm<sup>-1</sup>. Later, in 1997, Pine

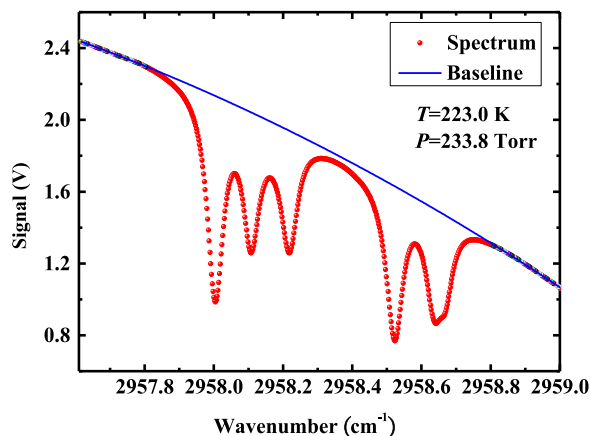


**Fig. 2.** Spectrum of  $N_2 + {}^{12}CH_4$  and corresponding base line. The blue base line was obtained by least squares fitting to a third-order polynomial. (For interpretation of the references to color in this figure legend, the reader is referred to the web version of this article.)

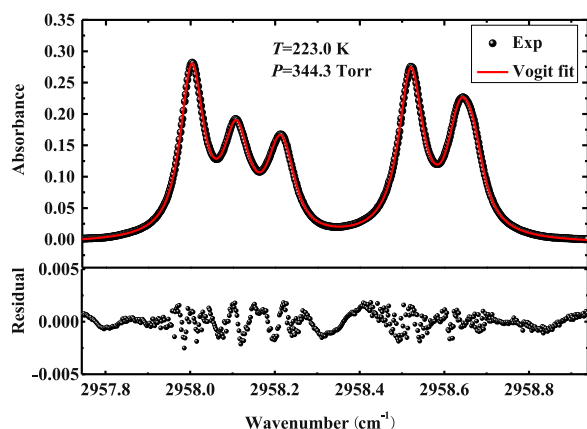


**Fig. 3.** Spectrum of air +  ${}^{12}CH_4$  and fits of Voigt profile (solid line). The top panel shows the measured (in dotted line) and calculated (in solid line) line profiles with a multi-peak fitting program. The lower panel shows the corresponding fitting residuals.

**Table 1**

Summary of experimental conditions of  $CH_4$  spectra analyzed in this work.

Temperature (K)	Broadening gas	Pressure range (Torr)
$296.0 \pm 0.3$	Air	50.95–287.8
$251.0 \pm 0.2$	Air	70.3–299.9
$223.0 \pm 0.2$	Air	79.6–344.3
$198.0 \pm 0.2$	Air	80.64–307.7
$173.0 \pm 0.3$	Air	72.83–290.9
$296.0 \pm 0.1$	$N_2$	84.37–294.6
$251.0 \pm 0.2$	$N_2$	58.47–273.8
$223.0 \pm 0.3$	$N_2$	69.39–293.5
$198.0 \pm 0.3$	$N_2$	73.94–305.5
$173.0 \pm 0.3$	$N_2$	80.1–294.4

Note: The partial pressure of  $CH_4$  in the mixture gases was always less than 0.5 Torr in this study ( $CH_4$ +air and  $CH_4$ + $N_2$  mixtures). For 296 K, the room temperature was controlled by an air conditioner.

[14] measured the  $N_2$ - and Ar-broadened spectra of the allowed  $P$ - and  $R$ -branch manifolds for  $J \leq 10$  in the  $\nu_3$  band of  $CH_4$  by using a difference-frequency generation

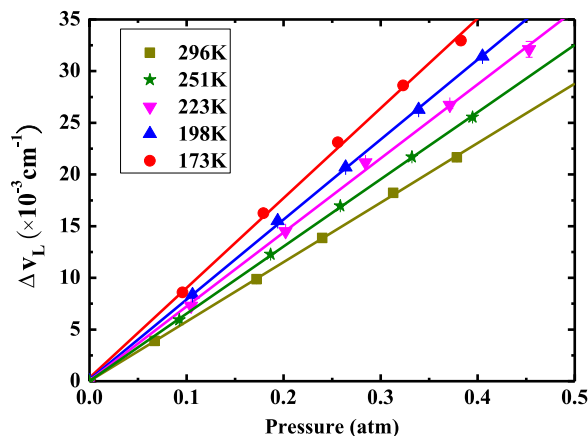


**Fig. 4.** Air pressure-induced half-widths of the  $CH_4$  line at  $2958.017263 \text{ cm}^{-1}$  derived from a linear fit of the absorption spectra of  $CH_4$ -air mixtures at various pressures and temperatures. The slope of the regression line through each set of symbols corresponds to the broadening coefficient in  $\text{cm}^{-1} \text{ atm}^{-1}$  at that temperature.

(DFG) spectrometer based on the difference-frequency of two dye-lasers. In 2000, the Speed-dependent broadenings and shifts have been reinvestigated for this band of  $CH_4$  perturbed by Ar and  $N_2$  using a multispectrum fitting analysis. Here, we compared our broadening coefficients at room temperature with those from Refs. [13–15].

Fig. 6 compares the  $N_2$ -broadening coefficients of six transitions at room temperature. The figure shows that for the first three transitions (P6 A1 1, P6 F1 1, P6 F2 2), our results are in good agreement with the previous studies within  $-5.4\%$   $\{(\text{Present work}-\text{other results})/(\text{other results}) \times 100\}$  with those from Refs. [13–15]. For the P6 A2 1, P6 F2 1, our results are close to Ref. [14] and Ref. [15], the maximum difference is less than  $-6.7\%$ . When compare our results (for P6 A2 1 and P6 F2 1) with those from Ref. [13], the difference becomes large (up to 13.3%). As to P6 E 1, our value is smaller than the other works, the differences are about  $-13.8\%$ ,  $-10.9\%$  and  $-11.5\%$  between our results and the measurements reported by Ref. [13], Ref. [14] and Ref. [15], respectively. It is difficult to explain this rather large difference for the last transition. However, it is interesting to note that, the broadening of methane in the  $\nu_3$  or other band was noted to be symmetry dependent, with some E transitions tending to be narrower than A or F Ref. [14 and reference therein].

It can be noticed that in Ref. [13], the  $N_2$ -broadening coefficients were obtained using a Fourier transform spectrometer with a limited resolution of  $0.01 \text{ cm}^{-1}$ , and the coefficients were retrieved from the best nonlinear least square fitting routine of the absorption lines assuming a Voigt lineshape while we were using very narrow laser source together with a nonlinear least-square fitting program based Voigt lineshape. In Ref. [14] and Ref. [15],  $N_2$ -broadening coefficients were measured using a DFG spectrometer with 1–5 MHz resolution. In Ref. [14], the absorption lines were fitted assuming a Rautian profile taking into account the Dicke narrowing effect. In the latter work, the speed dependent broadening and line

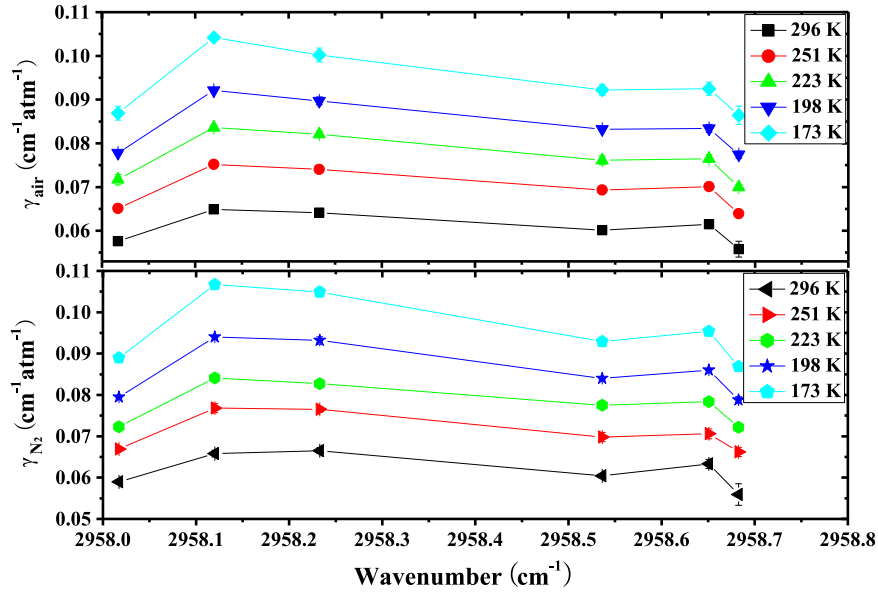


Fig. 5.  $N_2$ - and air-broadening coefficients as a function of the wavenumber at various temperatures for six transitions of  $\nu_3$  band of  $CH_4$ .

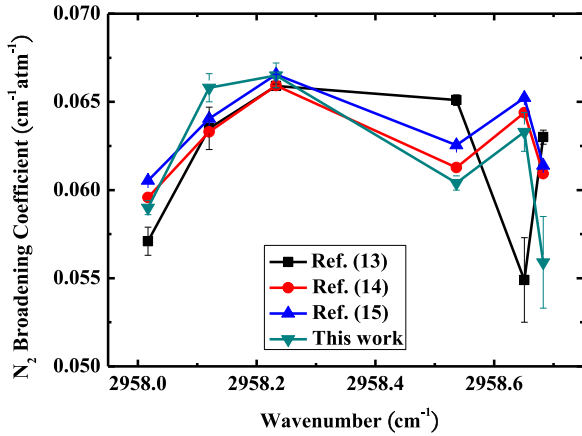


Fig. 6. The measured  $N_2$ -broadening coefficients of six transitions at room temperature from this work are plotted as a function of wavenumber and compared with other measurements (Refs. [13–15]).

mixing effects were also taken into account providing details of the theoretical line shape model used.

The air-broadening coefficients at room temperature from this study are summarized in Table 2 and compared with the data from other works. For the first line, the HITRAN value is higher than the present result (−6.6%), but we found our value was close to Ref. [13] with a discrepancy of about 2.7%. For the rest of the lines, HITRAN assumed the values from Ref. [13], so we only compared our values with those from HITRAN in the following text. For the transitions P6 F1 1, P6 F2 1 and P6 A2 1, the differences are −6%, −0.6% and 5.7%, respectively. For the last two lines, good agreement was not achieved, the differences are 13.3% and −10.7%, respectively. The possible reason for the difference may be caused by the different setup we used as we mentioned before. Since the  $N_2$ - and air-broadening coefficients were obtained using the same setup and our results agree well with the Refs. [14,15]

Table 2

Comparison of published air-broadening values for the six  $^{12}CH_4$  transitions with present measurements. The uncertainties in parentheses correspond to the errors obtained on the linear regression. These errors do not reflect errors arising from the systematic errors.

Line	$\nu_0^a$ ( $cm^{-1}$ )		$\gamma_0^{air}$ ( $10^{-3}cm^{-1}atm^{-1}$ )			
			HITRAN	This work	Ref. [13]	
$J$	$C$	$N^b$				
P6	A1	1	2958.017263	61.7	57.6(4)	56.0(10)
P6	F1	1	2958.120040	61.7	64.9(3)	61.7(14)
P6	F2	2	2958.232937	64.5	64.1(10)	64.5(2)
P6	A2	1	2958.536362	63.8	60.1(7)	63.8(3)
P6	F2	1	2958.650830	54.3	61.5(10)	54.3(22)
P6	E	1	2958.682546	62.5	55.8(18)	62.5(4)

<sup>a</sup> The assigned quantum numbers  $J$ ,  $C$ ,  $N$  represent the angular momentum, the rovibrational symmetry and the running number according to increasing energies within the polyads [23].

<sup>b</sup> The wave number values are extracted from HITRAN2012.

(except the last line), therefore, the presented results are believed to be reasonable.

#### 4.2. Temperature dependence exponent

The temperature dependence exponent  $n$  of the air- and  $N_2$ -broadening coefficients can be derived by using the Eq. (3) with the Lorentz width measured at room and low temperatures, which are listed in Table 3 together with the values from HITRAN database. The results are presented in Table 3. Fig. 7 shows the  $N_2$  temperature dependence of the transition at  $2958.120040\text{ cm}^{-1}$  as an example. For the temperature dependence exponents of our measurements, no significant trend was found. From Table 3 we can see that our air temperature dependence exponents are globally larger than those in HITRAN. (Note: these six temperature dependence exponents in HITRAN are from Antony et al. [20]). The average difference (12.2%) for the temperature

**Table 3**

Temperature exponent  $n$  for the air- and  $N_2$ -broadening coefficients of  $CH_4$  derived from the Voigt profile. The uncertainties in parentheses correspond to the errors obtained on the linear regression. These errors do not reflect errors arising from the systematic errors.

Line	$\nu_0(\text{cm}^{-1})$	$n$		HITR-AN Air	[(Exp-HITRAN)/ HITRAN]%
		This work			
		Air	$N_2$		
P6 A1 1	2958.017263	0.762(9)	0.772(24)	0.72	5.8%
P6 F1 1	2958.120040	0.876(8)	0.890(16)	0.72	21.7%
P6 F2 1	2958.232937	0.828(15)	0.844(26)	0.72	15.0%
P6 A2 1	2958.536362	0.792(16)	0.798(27)	0.72	10.0%
P6 F2 1	2958.650830	0.754(8)	0.773(18)	0.72	4.7%
P6 E 1	2958.682546	0.812(6)	0.817(28)	0.70	16.0%

Note: The wavenumber values are extracted from the HITRAN2012.

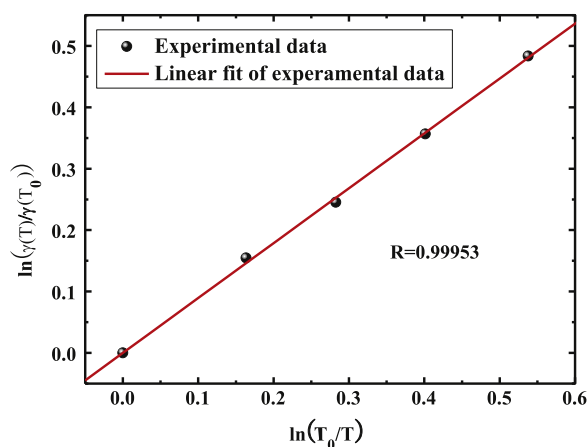


**Fig. 7.** Fits  $\ln[\gamma(T)/\gamma(T_0)]$  of as a function of  $\ln(T_0/T)$  for the transition at  $2958.120040 \text{ cm}^{-1}$  of  $CH_4$  using  $N_2$ -broadened half-widths measured over the range 173.0–251.0 K.

dependence exponents are slightly higher because our experiment temperature range is from 296.0 K to 173.0 K while the calculations of Ref. [20] were made at 225.0 and 296.0 K. Note that Antony et al. [20] compared their theoretical calculations of the temperature dependence exponents with those of earlier experiments [16–18]. It is however worth mentioning that the overall trend in their calculations shows that the theoretical temperature dependence exponents for the lines belonging to the  $\nu_3$  band of methane are  $\sim 17$ –48% smaller when compared to all experimental data (except the R (0) line measured by Varanasi [16]). Unfortunately, we did not find the  $N_2$  temperature dependence exponents for comparison.

## 5. Summary

The  $N_2$ - and air-broadening coefficients were measured from the analysis of the spectra of  $^{12}CH_4$  for six lines in the  $\nu_3$  band at room and low temperatures. The temperature dependence exponents have also been determined. The measurements were performed using a narrow linewidth diode laser operating at  $3.38 \mu\text{m}$  along with a home-made cryogenic cell. It was shown that for the two perturbers

(air and  $N_2$ ), the line broadening coefficients increase with the decrease in temperature for a given transition and all the air-broadening coefficients are slightly smaller than  $N_2$ -broadening coefficients. For air temperature dependence exponents, our results are globally larger than those in HITRAN with 12.2% discrepancy, while this is agreeing well with other experiments and calculations. The line parameters obtained in this work are credible through the detailed comparisons of our results and the previously published experimental data. These data will be helpful for the Earth's radiation balance and remote sensing of the Earth and outer planets atmospheres.

## Acknowledgements

This work was supported by the Young Scientists Fund of the National Natural Science Foundation of China (Grant no. 41205021) and the Youth Innovation Promotion Association of CAS under Grant no. 2015264. The authors are most grateful to Dr. Mingguo Sun and Dr. Guishi Wang for their help in some stages of this work and useful recommendations.

## Appendix A. Supplementary material

Supplementary data associated with this article can be found in the online version at <http://dx.doi.org/10.1016/j.jqsrt.2015.12.005>.

## References

- [1] Campargue A, Wang L, Kassi S, Mondelain D, Bézard B, et al. An empirical line list for methane in the 1.26–1.71  $\mu\text{m}$  region for planetary investigations ( $T=80$ –300 K). Application to Titan. *Icarus* 2012;219:110–28.
- [2] Strong K, Taylor FW, Colcutt SB, Remedios JJ, Ballard J. Spectral parameters of self- and hydrogen-broadened methane from 2000 to 9500  $\text{cm}^{-1}$  for remote sounding of the atmosphere of Jupiter. *J Quant Spectrosc Radiat Transf* 1993;50:363–429.
- [3] Bergamaschi P, Schupp M, Harris GW. High-precision direct measurements of  $^{13}CH_4/^{12}CH_4$  and  $^{12}CH_3D/^{12}CH_4$  ratios in atmospheric methane sources by means of a long-path tunable diode laser absorption spectrometer. *Appl Opt* 1994;33:7704–16.

- [4] Smith MAH, Rinsland CP, Devi VM, Benner DC. Temperature dependence of broadening and shifts of methane lines in the  $\nu_4$  band. *Spectrochim Acta A* 1992;48(9):1257–72.
- [5] Kassı S, Gao B, Romanini D, Campargue A. The near infrared (1.30–1.70  $\mu\text{m}$ ) absorption spectrum of methane down to 77 K. *Phys Chem Chem Phys* 2008;10:4410–9.
- [6] Gao B, Kassı S, Campargue A. Empirical low energy values for methane transitions in the 5852–6181  $\text{cm}^{-1}$  region by absorption spectroscopy at 81 K. *J Mol Spectrosc* 2009;253:55–63.
- [7] Sciamma-O'Brien E, Kassı S, Gao B, Campargue A. Experimental low energy values of  $\text{CH}_4$  transitions near 1.33  $\mu\text{m}$  by absorption spectroscopy at 81 K. *J Quant Spectrosc Radiat Transf* 2009;110:951–63.
- [8] Wang L, Kassı S, Campargue A. Temperature dependence of the absorption spectrum of  $\text{CH}_4$  by high resolution spectroscopy at 81 K: The region of the  $2\nu_3$  band at 1.66  $\mu\text{m}$ . *J Quant Spectrosc Radiat Transf* 2010;111:1130–40.
- [9] Deng LH, Gao XM, Cao ZS, Chen WD, Zhang WJ, Gong ZB. Empirical line intensities of methane at 1.51  $\mu\text{m}$ . *J Quant Spectrosc Radiat Transf* 2007;103:402–10.
- [10] Frankenbergh C, Warneke T, Butz A, Aben I, Hase F, Spietz P, Brown LR. Methane spectroscopy in the near infrared and its implication on atmospheric retrievals. *Atmos Chem Phys Discuss* 2008;8(3):10021–55.
- [11] Yi HM, Chen WD, Vicet A, Cao ZS, Gao XM, Nguyen-ba T, Jahjah M, Rouillard Y, Nöhle L, Fischer M. T-shape microresonator-based quartz-enhanced photoacoustic spectroscopy for ambient methane monitoring using 3.38  $\mu\text{m}$  antimonide-distributed feedback laser diode. *Appl Phys B* 2014;116:423–8.
- [12] Blake DR, Rowland FS. Continuing worldwide increase in tropospheric methane, 1978 to 1987. *Science* 1988;239:1129–31.
- [13] Benner DC, Devi VM, Smith MAH, Rinsland CP. Air-,  $\text{N}_2$ -, and  $\text{O}_2$ -broadening and shift coefficients in the  $\nu_3$  spectral region of  $^{12}\text{CH}_4$ . *J Quant Spectrosc Radiat Transf* 1993;50:65–89.
- [14] Pine AS.  $\text{N}_2$  and Ar broadening and line mixing in the P and R branches of the  $\nu_3$  band of  $\text{CH}_4$ . *J Quant Spectrosc Radiat Transf* 1997;57:157–76.
- [15] Pine AS, Gabard T. Speed-dependent broadening and line mixing in  $\text{CH}_4$  perturbed by Ar and  $\text{N}_2$  from multispectrum fits. *J Quant Spectrosc Radiat Transf* 2000;66:69–92.
- [16] Varanasi P. Air-broadened line widths of methane at atmospheric temperatures. *J Quant Spectrosc Radiat Transf* 1975;15(3):281.
- [17] Devi VM, Fridovich B, Jones GD, Strengths Snyder DGS, and Lorentz broadening coefficients for spectral lines in the  $\nu_3$  and  $\nu_2 + \nu_4$  bands of  $^{12}\text{CH}_4$  and  $^{13}\text{CH}_4$ . *J Mol Spectrosc* 1983;97:333–42.
- [18] Mondelain D, Payan S, Deng W, Camy-Peyret C, Hurtmans D, Mantz AW. Measurement of the temperature dependence of line mixing and pressure broadening parameters between 296 and 90 K in the  $\nu_3$  band of  $^{12}\text{CH}_4$  and their influence on atmospheric methane retrievals. *J Mol Spectrosc* 2007;244:130–7.
- [19] Rothman LS, Gordon IE, Babikov Y, Barbe A, Benner DC, et al. The HITRAN2012 molecular spectroscopic database. *J Quant Spectrosc Radiat Transf* 2013;130:4–50.
- [20] Antony BK, Niles DL, Wroblewski SB, Humphrey CM, Gabard T, Gamache RR.  $\text{N}_2$ -,  $\text{O}_2$ - and air-broadened half-widths and line shifts for transitions in the  $\nu_3$  band of methane in the 2726- to 3200- $\text{cm}^{-1}$  spectral region. *J Mol Spectrosc* 2008;251:268–81.
- [21] Ma HL, Sun MG, Cao ZS, Huang YB, Wang GS, Gao XM, Rao RZ. Cryogenic cell for low temperature spectral experiments of atmospheric molecules. *Opt Precis Eng* 2014;22:2617–21.
- [22] Gharavi M, Buckley SG. Diode laser absorption spectroscopy measurement of linestrengths and pressure broadening coefficients of the methane  $2\nu_3$  band at elevated temperatures. *J Mol Spectrosc* 2005;229:78–88.
- [23] Rothman LS, Jacquemart D, Barbe A, Benner DC, Birk M. The HITRAN2004 molecular spectroscopic database. *J Quant Spectrosc Radiat Transf* 2005;96:139–204.